International Journal of Advanced Science and Technology
Vol. 29, No. 6, (2020), pp. 4850 - 4861

Quality Grading of Dehazed Images Through Visibility Index

Diwakar Agarwal

Department of Electronics and Communication, GLA University, Mathura, India
diwakar.agarwal@gla.ac.in

Abstract

The foggy or hazy weather condition degrades the resolution and contrast of the acquired outdoor scene object. This leads to the poor visibility and necessitates the use of an image dehazing algorithm for the visibility enhancement of the captured images. This paper presents the proposed method to quantify the quality of the dehazed images in order to measure the effectiveness of the applied dehazing algorithm. In this paper, an algorithm based on Dark Channel Prior (DCP) and guided filter is implemented for image dehazing. The DCP is based on the characteristic of dark pixels in that the pixels hold low intensity value in atleast one color channel of the haze-free outdoor images. The transmission map so obtained from dark channel prior is refined by applying guided filter. The dominant advantage of using guided filter is its capability to keep sharp details while upholding the color quality. The proposed algorithm is tested over the number of hazy natural images. The image quality transition from an input hazy image to an output dehazed image is evaluated in terms of Visibility Index (VI). The dehazed image falls into either three quality grades; medium, slight and non-hazy. The experimental results so achieved are remarkable to show the quite difference between the quality of input and output images of the applied dehazing algorithm.

Keywords: *dark channel, dehazing, depth map, guided filter, restoration, visibility index*

1. Introduction

Haze, fog and smoke are caused due to the suspension of water droplets or ice crystals in the low-lying air near the earth's surface [1]. This leads to the absorption and scattering of tiny particles which eventually results into the degradation of the visibility of outdoor scene images. The degradation not only effects consumer and commercial photography but also many high-level computer vision tasks; some of them includes object detection, tracking, video surveillance, etc. According to the global road safety body; International Road Federation (IRF), the large number of road fatalities are happened in foggy weather conditions [2]. The most obvious reason behind this is the limited employability of the image dehazing modules in automobiles and railways.

Image dehazing methods are broadly classified into two categories: multiple image-based and single-image based. Earlier methods [3-7] of image dehazing required multiple instances of the same scene for their implementation. These methods were suffered by the limited application in online image dehazing. On the other hand, single image-based dehazing methods requires a single image at its input and utilizes the physical characteristics of an image. Number of algorithms [8-17] which are based on the single image is available in the literature. These algorithms have implemented the spatial domain techniques of image restoration. The stack of spatial domain techniques includes several methods such as depth map estimation, filtering, enhancement, meta-heuristics methods and fusion.

ISSN: 2005-4238 IJAST

In this work, image dehazing is performed by implementing the well-known single image-based dehazing algorithm proposed by He et al [10]. In this method, an image dehazing model was considered and the dark channel prior was estimated based on the assumption that the dark pixels possess low intensity value very close to zero in atleast one of the color channel within a patch of haze-free images. An atmospheric light and the refined transmission map were then determined. In this paper, the transmission map is refined by using the guided filter. The dehazed image is then obtained after applying the closed form formulae utilizing the atmospheric light and the refined transmission map. To assess the quality improvement from the input hazy image to the output dehazed image is not the matter of subjective analysis since different persons have their own visual perception. Thus, the main contributions of this paper are (i) Use of guided filter with the DCP estimation for image dehazing (ii) Defining the judging criterion based on the calculated visibility index in order to assess the quality of the dehazed images. The proposed algorithm is applied on the number of hazy natural images, some of them downloaded from FRIDA database [18] and some images are shot by Vivo Y17 13 MP camera.

The rest of the paper is organised as follows: section 2 presents the related work, section 3 describes the proposed algorithm, section 4 shows the experimental results and discussion, conclusion is provided in section 5.

2. Related work

In any image dehazing technique, the depth map estimation is one of the most important steps which makes easy the whole dehazing process. However, knowing the depth map before is not possible for real time applications since the transmission depends upon the scene depth which is unknown and varies with the weather conditions. Tan [8] and Kawakami et al. [19] have proposed the use of contrast as one of the distinguishable characteristics between hazy and dehazed image after finding the high contrast values in haze-free images. This method maximized the locally defined contrast of the input hazy image but in return of producing blocking artifacts in the output. Fatal et al. [9] estimated the optical transmission in constant-albedo and multi-albedo images with an underlying assumption that the transmission was statistically uncorrelated with the shading surface of the scene. This method was not applicable to thick hazed images. He et al. [10] have proposed a simple and an operative approach of image dehazing based on DCP. This technique was composed of the estimation of atmospheric light, transmission map, transmission map refinement and dehazed image construction. Several algorithms [11-17] were then evolved by considering DCP as one of the crucial steps in their implementation. These algorithms were differing each other in that, they were applied different methods at each step of the basic DCP estimation proposed by He et al. [10]. However, these algorithms were suffered by the halo artifacts and color distortion. In order to improve the processing time of image restoration and to reduce colour artifacts, some wavelet transform-based algorithms [20, 21] were developed. The computational speed was further improved in modified versions by combining wavelet transform and DCP estimation [22, 23]. Number of algorithms were also utilized image enhancement techniques such as histogram equalization [24], weighted histograms [25], Bi-histogram modification [26] etc. These techniques were suffered by the over enhancement and saturated pixel issues. An output of image restoration was improved from coarse to refined by applying filtering-based image dehazing methods such as median filter [27], L2-norm with guided filter [28], weighted guided image filter [29], bilateral filter [30] etc. These methods were suffered from computational complexity and dependency on the accurate estimation of various priors. Some algorithms [31-34] have proposed the design of machine learning based on supervised learning models to determine the depth map by training the models with several

ISSN: 2005-4238 IJAST

hazy and dehazed images. The linear model was proposed in [31], two-layer Gaussian regression was introduced in [32], DehazeNet in [33] and kernel regression model was utilized in [34].

3. Proposed method

The block diagram representation of an image dehazing method used in the proposed algorithm is shown in fig 1. It consists of mainly two broad steps: DCP estimation and dehazed image construction. An atmospheric light and transmission map are estimated from the dark channel prior. The transmission map is refined by using guided filter which later combined with the atmospheric light to generate dehazed image.

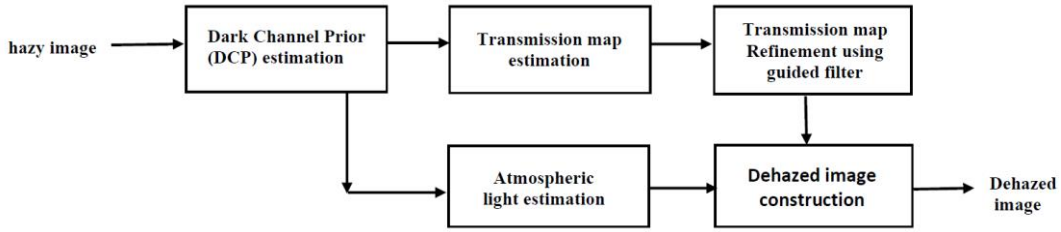

Figure 1. Block diagram representation of DCP based image dehazing method

3.1. DCP Estimation

An image hazing model which was described in [35, 36] is given by (1)

$$I(m,n) = J(m,n)t(m,n) + A(1 - t(m,n)) \quad (1)$$

where, I is the hazy image, J is the scene radiance or haze-free image, t is the transmission map, A is the global atmospheric light and (m, n) is the image spatial coordinate. The transmission map t is given by (2)

$$t(m,n) = e^{-\beta d(m,n)} \quad (2)$$

where β is the atmospheric scattering coefficient ($\beta \approx 0$ in case of clear weather condition) and d is the scene depth. The first term $J(m,n)t(m,n)$ in Eq. (1) defines a direct attenuation of the scene radiance which decreases exponentially when the scene depth increases. In contrast, the second term $A(1 - t(m,n)$ which is called the airlight increases with the increasing scene depth. The main purpose of the image hazing model is to obtain $J(m,n)$ from $I(m,n)$, A and $t(m,n)$. The $J(m,n)$ is derived from Eq. (1) which is given by (3)

$$J(m,n) = \frac{I(m,n) - A}{t(m,n)} + A \quad (3)$$

The global atmospheric light A and transmission map $t(m,n)$ are determined from the DCP estimation. The evaluation of the dark channel is based on the property that the dark pixels of the haze-free images except sky regions have intensity value close to zero in atleast one color channel within an image patch. The low intensity values in non-sky regions are occurred due to (a) shades of roadside cars, buildings, leaves, trees (b) colourful and dark

ISSN: 2005-4238 IJAST

objects or surfaces. Thus, the dark pixel intensity value at the spatial location (m, n) in an arbitrary image J is determined by using (4)

$$J^{dark}(m,n) = \min_{y\in\Omega(m,n)}\left(\min_{c\in\{r,g,b\}} J^c(y)\right) \tag{4}$$

where, $\Omega(m,n)$ is an image patch centered at the spatial location (m, n) and J^c is the color channel. Therefore, the pixel intensity value in the dark channel image J^{dark} at (m, n) is defined as the minimum intensity value in $\Omega(m,n)$ among three channels $\{r, g, b\}$. If J is the haze-free image then,

$$J^{dark} \to 0 \tag{5}$$

In contrast to haze-free images, hazy images are brighter due to the additive airlight and low transmission map. The dark channel of a hazy image is a good approximation of the thickness of the haze since it owns the high intensity values in the highly dense haze regions. Therefore, this property is used to determine atmospheric light and transmission map.

3.2. Transmission Map Estimation

Given the atmospheric light A, the normalization of the Eq. (1) at each color channel c independently is given by (6)

$$\frac{I^c(m,n)}{A^c} = t(m,n)\frac{J^c(m,n)}{A^c} + 1 - t(m,n) \tag{6}$$

Considering the local image patch $\Omega(m,n)$, the minimum intensity in each color channel and in all pixels of $\Omega(m,n)$ is given by (7)

$$\min_{y\in\Omega(m,n)}\left(\min_c \frac{I^c(y)}{A^c}\right) = \tilde{t}(m,n)\min_{y\in\Omega(m,n)}\left(\min_c \frac{J^c(m,n)}{A^c}\right) + (1-\tilde{t}(m,n)) \tag{7}$$

where, $\tilde{t}(m,n)$ is the transmission map which is constant within an image patch. The following term in Eq. (7) is the dark channel J^{dark} as given in Eq. (4) which is zero since J is the scene radiance.

$$J^{dark}(m,n) = \min_{y\in\Omega(m,n)}\left(\min_c \frac{J^c(m,n)}{A^c}\right) = 0 \tag{8}$$

Put Eq. (8) in Eq. (7) and thus transmission map $\tilde{t}(m,n)$ is obtained as

$$\tilde{t}(m,n) = 1 - \min_{y\in\Omega(m,n)}\left(\min_c \frac{I^c(y)}{A^c}\right) \tag{9}$$

Since the brightness of the sky region in a hazy image is equivalent to the atmospheric light A, therefore,

$$\min_{y\in\Omega(m,n)}\left(\min_c \frac{I^c(y)}{A^c}\right) \to 1 \tag{10}$$

and the transmission map $\tilde{t}(m,n) \to 0$ in the sky regions. This compensates the non-applicability of the DCP in the sky regions of haze-free images.

ISSN: 2005-4238 IJAST

3.3. Transmission Map Refinement

The next step is the transmission map refinement which was performed by the number of methods available in the literature such as Gaussian filter, bilateral filter, soft matting etc. In the proposed method, the transmission map is refined by applying the guided filter. The guided filter utilized the hazy image as the guidance image. Therefore, the refined transmission map preserves similar sharpness level comparable to the hazy image and doesn't include false color texture. The refined transmission map is given by (11)

$$\hat{t}(x) = \bar{a}_x \tilde{t}(x) + \bar{b}_x \tag{11}$$

where, $\bar{a}_x$ and $\bar{b}_x$ are the average of all coefficients obtained within an image patch $\Omega(x)$ obtained at the pixel location *x* i.e. at (*m*, *n*).

$$\bar{a}_x = \frac{1}{|w|}\sum_{y\in\Omega(x)} a_x \tag{12}$$

$$\bar{b}_x = \frac{1}{|w|}\sum_{y\in\Omega(x)} b_x \tag{13}$$

where, $|w|$ is the number of pixels in $\Omega(x)$. The coefficients a_x and b_x are given by

$$a_x = \frac{\frac{1}{|w|}\sum_{y\in\Omega(x)} I_y \tilde{t}(y) - \mu_x \bar{t}(x)}{\sigma_x^2 + \varepsilon} \tag{14}$$

$$b_x = \bar{t}(x) - b_x \mu_x \tag{15}$$

where $\bar{t}(x)$ is given by

$$\bar{t}(x) = \frac{1}{|w|}\sum_{y\in\Omega(x)} \tilde{t}(y) \tag{16}$$

3.4. Atmospheric Light Estimation

The main idea behind the estimation of the atmospheric light *A* is to detect most blurred region in the hazy image. This region is detected with the help of DCP since as stated above, the dark channel prior provides a good estimation of the haze thickness. At first, top 0.1% bright pixels of the dark channel of a hazy image are determined. Then among these pixels, the highest intensity pixels in the input image are located. In fact, these pixels composed the most blurred region and considered as an atmospheric light.

3.5. Dehazed Image Construction

After estimating the refined transmission map $\hat{t}$ and the atmospheric light *A*, the dehazed image *J* is constructed by following the Eq. (3). The transmission map *t* is replaced by the estimated transmission map $\tilde{t}$. The possibility of $\tilde{t} = 0$ cannot be ignored since it will result into noisy dehazed image. Thus, to avoid this condition, the term t_0 is included in the denominator of the Eq. (3). The value of t_0 is chosen as 0.1 empirically. The modified equation for constructing the dehazed image is given by (17)

$$J(m,n) = \frac{I(m,n) - A}{\max\left(\tilde{t}(m,n), t_0\right)} + A \tag{17}$$

ISSN: 2005-4238 IJAST

3.6. Dehazed Image Grading

It is necessary to determine the quality of the output dehazed image in order to know that how much amount of haziness has removed after passing an input hazy image into an image dehazing model. The quality determination is not dependent on any subjective criterion since different persons have different human perception. This paper proposes the quantification of the quality grades assignment to the output dehazed images in terms of the visibility index. The visibility index is defined by *VI* is given by (18)

$$VI = \frac{\sqrt{std}(pixel\ range)^2}{100(mean)} \tag{18}$$

where, std is the standard deviation of the intensities in an image, $pixel\ range$ is the range and $mean$ is the average value of the intensities in an image. Table 1 shows the judging criterion defining the quality grading of an image with respect to the range of *VI*.

Table 1. Range of visibility index

Range of VI	Image quality grading
0-25	Medium hazy
25-45	Slight hazy
>45	Non-hazy

4. Experimental Results

For the implementation of the proposed method, a database of natural hazy images is formed which includes some images of FRIDA database [18] and some images which are shot by Vivo Y17 13 MP camera. Figure 2 shows the first 12 example images of the database which are used as an input to the proposed method. The corresponding dehazed outputs are shown in fig 3. Table 2 shows the value of the mean, standard deviation, range and VI of input hazy images and Table 3 shows the value of same parameters for the corresponding output dehazed images.

Table 2. Visibility Index of input hazy Images

S.No	Figure No.	Average	Standard deviation	Range	Visibility Index
1.	Fig 2(a)	155.86	35.48	228	19.86
2.	Fig 2(b)	163.48	23.25	189	10.53
3.	Fig 2(c)	202.24	31.22	118	3.84
4.	Fig 2(d)	134.49	51.85	213	24.29

ISSN: 2005-4238 IJAST

Table 2. Visibility Index of input hazy Images (Continued)

S.No	Figure No.	Average	Standard deviation	Range	Visibility Index
5.	Fig 2(e)	118.43	41.98	254	35.29
6.	Fig 2(f)	189.62	20.94	161	6.255
7.	Fig 2(g)	130.56	66.54	215	28.88
8.	Fig 2(h)	119.48	29.16	146	9.63
9.	Fig 2(i)	104.08	48.52	205	28.12
10.	Fig 2(j)	164.66	42.63	233	21.52
11.	Fig 2(k)	153.98	67.92	253	34.34
12.	Fig 2(l)	120.03	65.76	254	43.58

Table 3. Visibility Index of the output dehazed Images

S.No	Figure No.	Average	Standard deviation	Range	Visibility Index
1.	Fig 3(a)	84.40	55.56	223	43.91
2.	Fig 3(b)	126.81	37.97	234	39.10
3.	Fig 3(c)	142.09	53.39	191	18.76
4.	Fig 3(d)	96.98	62.53	219	39.10
5.	Fig 3(e)	65.49	37.76	255	61.01
6.	Fig 3(f)	108.94	35.69	255	35.66
7.	Fig 3(g)	93.77	66.47	229	45.59
8.	Fig 3(h)	100.15	39.41	183	20.99
9.	Fig 3(i)	72.53	37.64	212	38.01

ISSN: 2005-4238 IJAST

Table 3. Visibility Index of the output dehazed Images (Continued)

S.No	Figure No.	Average	Standard deviation	Range	Visibility Index
10.	Fig 3(j)	107.34	61.69	254	47.20
11.	Fig 3(k)	101.44	67.73	255	52.75
12.	Fig 3(l)	67.13	50.01	254	67.95

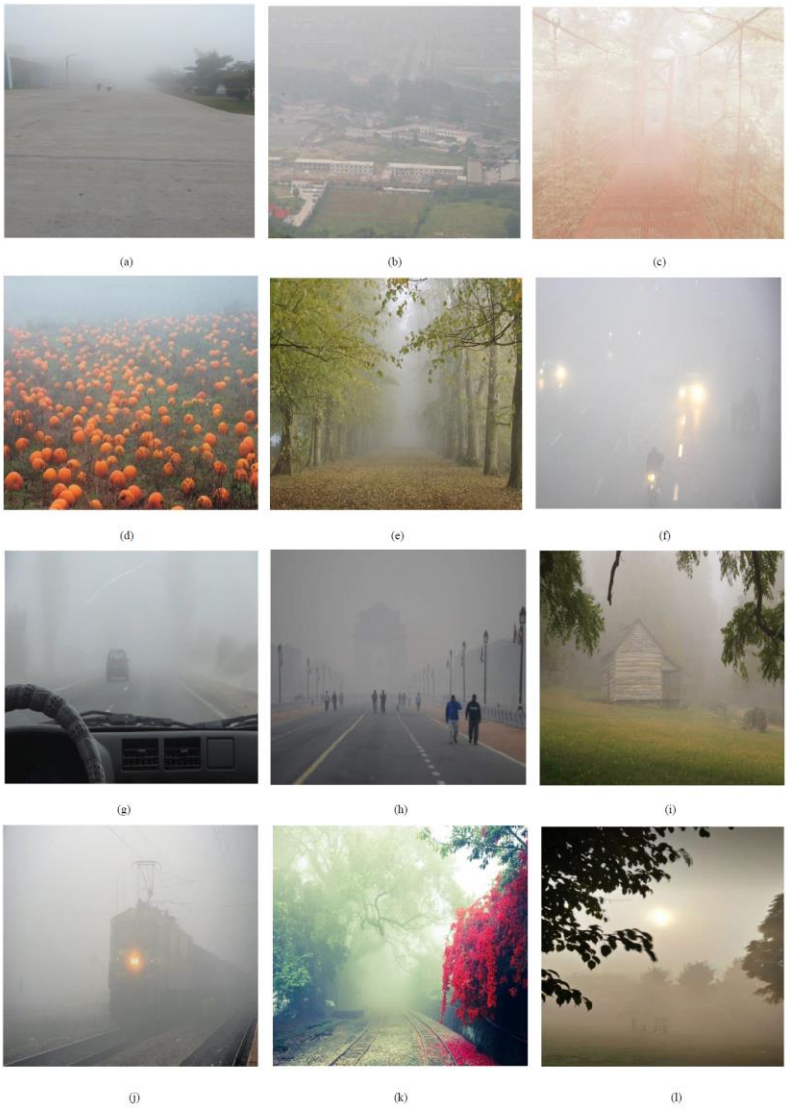

Figure 2. (a)-(l) Input hazy images

ISSN: 2005-4238 IJAST

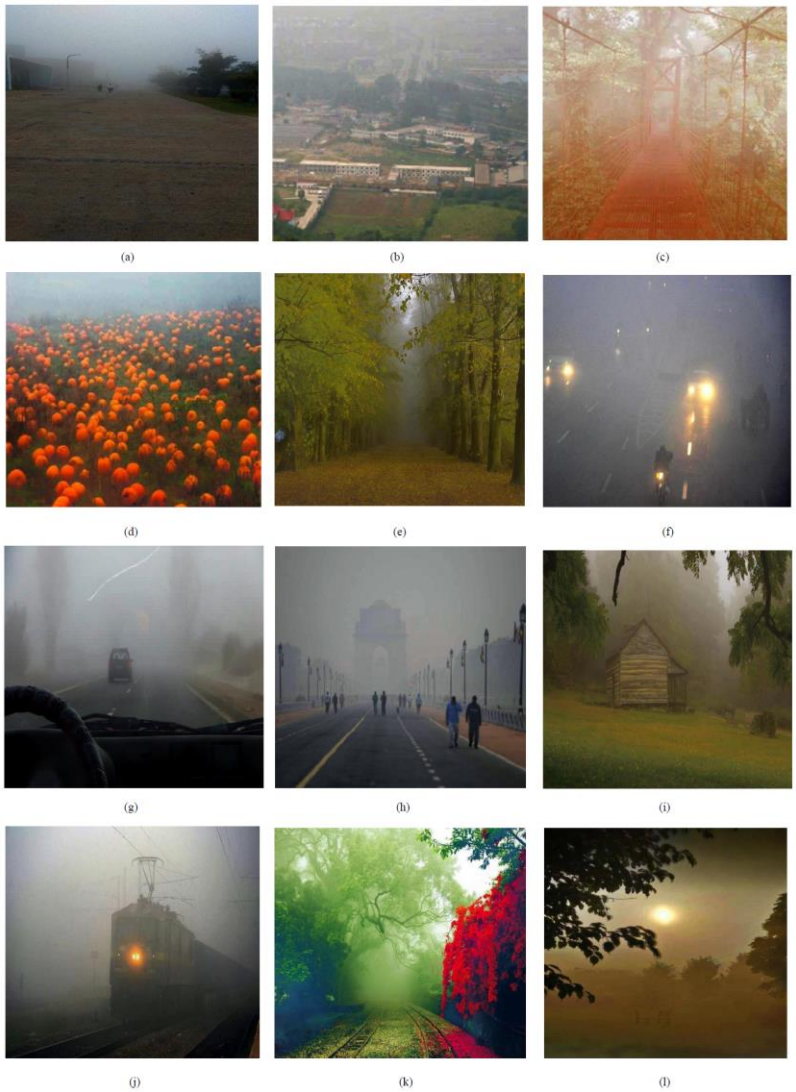

Figure 3. (a)-(l) output dehazed images corresponding to the input hazy images of fig 2

The dehazing increases the visibility index of the output images in comparison to the input images. The values of VI in table 3 is more than the corresponding values of VI in table 2. This increased visibility index shows the improvement in the quality of the dehazed image. Table 4 shows the transition from input image quality to the output image quality in accordance with the VI values fall in the pre-defined range as given in table 1.

The quality transition in table 4 reveal the effectiveness of the applied dehazing algorithm in that the medium hazy input images are transformed into slight and non-hazy output images; also, slight hazy input images are transformed into non-hazy output images.

ISSN: 2005-4238 IJAST

Table 4. Transition in the quality of images from input to output

Figure No.	Input images		Figure No.	Output images		Quality transition
	VI	Quality		VI	Quality	
Fig 2(a)	19.86	Medium hazy	Fig 3(a)	43.91	Slight hazy	Medium to Slight
Fig 2(b)	10.53	Medium hazy	Fig 3(b)	39.10	Slight hazy	Medium to Slight
Fig 2(c)	3.84	Medium hazy	Fig 3(c)	18.76	Medium hazy	No change
Fig 2(d)	24.29	Medium hazy	Fig 3(d)	39.10	Slight hazy	Medium to Slight
Fig 2(e)	35.29	Slight hazy	Fig 3(e)	61.01	Non-hazy	Slight to Non-hazy
Fig 2(f)	6.25	Medium hazy	Fig 3(f)	35.66	Slight hazy	Medium to Slight
Fig 2(g)	28.88	Slight hazy	Fig 3(g)	45.59	Non-hazy	Slight to Non-hazy
Fig 2(h)	9.63	Medium hazy	Fig 3(h)	20.99	Medium hazy	No change
Fig 2(i)	28.12	Slight hazy	Fig 3(i)	38.01	Slight hazy	No change
Fig 2(j)	21.52	Medium hazy	Fig 3(j)	47.20	Non-hazy	Medium to Non-hazy
Fig 2(k)	34.34	Slight hazy	Fig 3(k)	52.75	Non-hazy	Slight to Non-hazy
Fig 2(l)	43.58	Slight hazy	Fig 3(l)	67.95	Non-hazy	Slight to Non-hazy

However, three input images fig 2(c), fig 2(h) and fig 2(i) and their corresponding output images fig 3(c), fig 3(h) and fig 3(i) exhibit no change in the type of the haziness present in the images. This is due to the invalidity of the dark channel prior since the scene object of these images is equivalent to the atmospheric light and no shadow is projected on them.

5. Conclusion

The effectiveness of any image dehazing algorithm is dependent on the considerable improvement in the quality of the input hazy images. In this paper, a judging criterion to

ISSN: 2005-4238 IJAST

evaluate the quality (medium, slight and non-hazy) of the output dehazed images was presented. The image dehazing was performed by combining the dark channel prior and guided filter. The estimation of dark channel prior and its utilization with image hazing model provides a simple and effective haze removal. The refinement of the transmission map was accomplished with the help of guided filter. The guided filter is more generic in handling some applications and works better on edges. Since the image dehazing has a wide application area (military, underwater vision, air traffic control, night vision etc), it is necessary that illumination and the color characteristics of the dehazed images should be restored and preserved. As future aspects, advance dehazing models can be design for real time scenes which are generally observed in a moving vehicle. Definitely, machine learning and artificial intelligence-based models could be helpful for those applications which demands on-the-spot visibility enhancement.

References

[1] I. Gultepe, Editor, "Fog and boundary layer clouds: fog visibility and forecasting", Springer Science & Business Media, **(2008)**.
[2] www.newindianexpress.com/nation/2018/jan/04/global-road-body-international-road federation-for - mandatory-fog-lights-in-vehicles-1744760.html, Accessed on 24 April, 2020.
[3] Y.Y. Schechnner, S.G. Narasimhan, S.K. Nayar, "Polarization-based Vision through Haze", Appl. Optics., vol. 42, no. 3, **(2003),** pp. 511–525.
[4] Y.Y. Schechnner and S.G. Narasimhan, "Instant Dehazing of Images Using Polarization", Proceedings of IEEE Computer Society Conference on Computer Vision and Pattern Recognition, Kauai, **(2001)**, pp. 25–332.
[5] S. Shwartz, E. Namer, Y.Y. Schechner, "Blind Haze Separation", Proceedings of IEEE Computer Society Conference on Computer Vision and Pattern Recognition, Anchorage, **(2006)**, pp. 1984–1991.
[6] S.G. Narasimhan and S.K. Nayar, "Contrast Restoration of Weather Degraded Images", IEEE Trans. Pattern Anal. Mach. Intell., vol. 25, no. 6, **(2003)**, pp. 713–724.
[7] S.K. Nayar and S.G. Narasimhan, "Vision in Bad Weather", Proceedings of the 7th IEEE International Conference on Computer Vision, Kerkyra, **(1999)**, pp. 820–827.
[8] R.T. Tan, "Visibility in Bad Weather from a Single Image", Proceedings of IEEE Computer Society Conference on Computer Vision and Pattern Recognition, Anchorage, **(2008)**, pp. 1–8.
[9] R. Fattal, "Single Image Dehazing", ACM Trans. Graph., vol. 72, no. 3, **(2008)**, pp. 72:1-72:9.
[10] K. He, J. Sun, X. Tang, "Single image haze removal using dark channel prior", IEEE Trans. Pattern Anal. Mach. Intell., vol. 33, no. 12, **(2010)**, pp. 2341–2353.
[11] S.C. Huang, B.H. Chen, W.J. Wang, "Visibility Restoration of Single Hazy Images Captured in Real-World Weather Conditions", IEEE Trans. Circuits Sys., Video Tech., vol. 24, no.10, **(2014)**, pp. 1814–1824.
[12] Y. Linan, P. Yan, Y. Xiaoyuan, "Video Defogging Based on Adaptive Tolerance", TELKOMNIKA Indonesian Journal of Elec., vol. 10, no. 7, **(2012)**, pp. 1644–1654.
[13] H. Xu, J. Guo, Q. Liu, L. Ye, "Fast Image Dehazing Using Improved Dark Channel Prior, Proceedings of International Conference on Information Science and Technology, Hubei, **(2012)**, pp. 663–667.
[14] Z. Tan, X. Bai, A. Higashi, "Fast Single Image Defogging". FUJITSU Sci. Tech. J., vol. 50, no. 1, **(2014)**, pp. 60–65.
[15] C. Xiao, J. Gan, "Fast Image Dehazing Using Guided Joint Bilateral Filter", Vis. Comput., vol. 28, no. 6-8, **(2012)**, pp. 713–721.
[16] H. Yang, J. Wan, H. Yang, J. Wang, H. Yang, J. Wang, "Color Image Contrast Enhancement by Co-occurrence Histogram Equalization and Dark Channel Prior", Proceedings of 3rd International Congress on Image and Signal Processing, Yantai, **(2010)**, pp. 659–663.
[17] M. S. Sandeep, "Remote sensing image dehazing using guided filter", International Journal of Research Studies in Computer Science and Engineering., vol. 1, no. 3, **(2014)**, pp. 44–49.
[18] J. P. Tarel, N. Hautiere, A. Cord, D. Gruyer, H. Halmaoui, "Improved Visibility of Road Scene Images Under Heterogeneous Fog", In 2010 IEEE Intelligent Vehicles Symposium, **(2010)**, pp. 478-485.
[19] R. Kawakami, H. Zhao, R. T. Tan, K. Ikeuchi, "Camera Spectral Sensitivity and White Balance Estimation from Sky Images", Int J Comput Vis., vol. 105, no. 3, **(2013)**, pp. 187–204.
[20] Z. Rong and W. L. Jun, "Improved Wavelet Transform Algorithm for Single Image Dehazing", Optik Int J Light Electron Opt., vol. 125, no. 13, **(2014)**, pp. 3064–3066.
[21] Y. Yang, Z. Fu, X. Li, C. Shu, X. Li, "A Novel Single Image Dehazing Method", Proceedings of International Conference on Computational Problem-Solving, **(2013)**, pp 275–278.

ISSN: 2005-4238 IJAST

[22] A. Khmag, S. Al-Haddad, A. R. Ramli, B. Kalantar, "Single Image Dehazing Using Second Generation Wavelet Transforms and Mean Vector l2-Norm", The Visual Computer., vol. 34, no. 5, (2018), pp. 675-688.
[23] Z. Wang and Y. Feng, "Fast Single Haze Image Enhancement", Comput Electr Eng., vol. 40, no. 3, **(2014)**, pp. 785–795.
[24] X. Fu, J. Wang, D. Zeng, Y. Huang, X. Ding, "Remote Sensing Image Enhancement Using Regularized-Histogram Equalization and DCT", IEEE Geosci Remote Sens Lett., vol. 12, no. 11, **(2015)**, pp. 2301–2305.
[25] S. He, Q. Yang, R. W. Lau, M. H. Yang, "Fast Weighted Histograms for Bilateral Filtering and Nearest Neighbor Searching", IEEE Trans Circ Syst Video Technol., vol. 26, no. 5, **(2016)**, pp. 891–902.
[26] A. S. A. Ghani and N. A. M. Isa, "Automatic System for Improving Underwater Image Contrast and Color through Recursive Adaptive Histogram Modification", Comput Electron Agric., vol. 141, **(2017)**, pp. 181–195.
[27] A. Kumari and S. K. Sahoo, "Fast Single Image and Video Deweathering Using Look-Up-Table Approach", AEU Int J Electron Commun., vol. 69, no. 12, **(2015)**, pp. 1773–1782.
[28] M. Ding and L. Wei, "Single Image Haze Removal Using the Mean Vector L2-Norm of RGB Image Sample Window," Optik Int J Light Electron Opt., vol. 126, no. 23, **(2015)**, pp. 3522–3528.
[29] Z. Li, J. Zheng, Z. Zhu, W. Yao, S. Wu, "Weighted Guided Image Filtering", IEEE Trans Image Process., vol. 24, no. 1, **(2015)**, pp. 120–129.
[30] W. Sun, H. Wang, C. Sun, B. Guo, W. Jia, M. Sun, "Fast Single Image Haze Removal via Local Atmospheric Light Veil Estimation", Comput Electr Eng., vol. 46, **(2015)**, pp. 371–383.
[31] Q. Zhu, J. Mai, L. Shao, "A Fast Single Image Haze Removal Algorithm Using Color Attenuation Prior", IEEE Trans Image Process., vol. 24, no. 11, **(2015)**, pp. 3522–3533.
[32] X. Fan, Y. Wang, X. Tang, R. Gao, Z. Luo, "Two-layer Gaussian Process Regression with Example Selection for Image Dehazing", IEEE Trans Circ Syst Video Technol., vol. 27, no. 12, **(2016)**, pp. 2505-2517.
[33] B. Cai, X. Xu, K. Jia, C. Qing, D. Tao, "DehazeNet: An End-to End System for Single Image Haze Removal", IEEE Trans Image Process. Vol. 25, no. 11, **(2016)**, pp. 5187–5198.
[34] C. H. Xie, W. W. Qiao, Z. Liu, W. H. Ying, "Single Image Dehazing Using Kernel Regression Model and Dark Channel Prior", Signal, Image and Video Processing., vol. 11, no. 4, **(2017)**, pp. 705-712.
[35] S. G. Narasimhan and S. K. Nayar, "Vision and the Atmosphere," Int'l J. Computer Vision., vol. 48, no. 3, **(2002)**, pp. 233-254.
[36] S. G. Narasimhan and S. K. Nayar, "Chromatic Framework for Vision in Bad Weather," Proc. IEEE Conf. Computer Vision and Pattern Recognition., vol. 1, **(2000)**, pp. 598-605.

ISSN: 2005-4238 IJAST